A Novel Acquisition Algorithm Based on PMF-apFFT for BOC Modulated Signals

YI PAN, TIANQI ZHANG, GANG ZHANG, AND ZHONGTAO LUO

School of Telecommunication and Information Engineering, Chongqing University of Posts and Telecommunications, Chongqing 400065, China

Corresponding author: Yi Pan (willboc@126.com)

ABSTRACT Large Doppler shifts are inherent to high-speed relative motion between receiver and satellite and are likely to cause major problems during the code phase acquisition due to the introduced frequency ambiguity. In order to solve the problem of acquisition for the binary offset carrier (BOC) modulated the signal with large Doppler shift, a novel acquisition algorithm based on partial matched filter-all phase fast Fourier transform (PMF-apFFT) is proposed in this paper. In this method, all phase processing was adopted to weaken the effect of spectrum leakage after partial correlation, and two dimensional parallel searching for Doppler frequency on different code phases was completed by the maximum value after the cumulative average exceeding the threshold. The theoretical analysis and simulation results show that the correct code phase search and high precision estimation of Doppler frequency can be completed by the proposed algorithm at the same time. Compared with the traditional PMF-FFT acquisition algorithm, the proposed algorithm has stronger anti-noise performance and a better detection probability, and it is suitable for the complex communication environment of strong noise and large Doppler shift.

INDEX TERMS Partial matched filter-all phase fast Fourier transform (PMF-apFFT), binary offset carrier (BOC) signal, acquisition, large Doppler shift.

I. INTRODUCTION

The contradiction, which is between the increasing demands of navigation frequency resource and the relatively limited frequency sharing ability of the binary phase shift keying (BPSK) modulated signal, has contributed to the wide application of binary offset carrier (BOC) modulation in the modern global navigation satellite system (GNSS) [1], [2]. More than 100 satellites, including GPS, GLONASS, GALILEO and BEIDOU systems, hovering in the sky, among which modern GPS, GALILEO and BEIDOU systems all use BOC modulation signals [3], [4].

The basic idea of BOC modulation is to add the periodic subcarrier modulation on the basis of BPSK signal, i.e., each PN spectrum code chip has been pre-modulated by periodic subcarriers. Meanwhile, the subcarrier modulation splits the main lobe of BOC signal power spectrum into two parts, it avoids overlapping with other traditional signals spectrum,

realizes spectrum sharing and solves the problems of compatibility and mutual interference among satellite navigation system thoroughly. In addition, compared with BPSK modulation signal, the main lobe width of (the same spreading code chip width) BOC modulation signal is smaller, which means advantages on acquisition performance, code tracking accuracy and inherent multipath resistance ability [5], [6].

The acquisition methods for BOC signal were proposed successively, from the perspective of time-frequency analysis, the cores of algorithm can be divided into time domain and frequency domain. Typical time domain algorithms are as follow: Auto-correlation Side-Peak Cancellation Technique (ASPeCT) [7], uses the auto-correlation function (ACF) and cross-correlation function (CCF) to construct a new correlation function, but the elimination of side peaks is not enough. Pseudo correlation Function (PCF) [8] algorithm combines local auxiliary signals and the received BOC signal to construct an unambiguous correlation function, it has a good applicability but peak value is low. In Sharp Reconstruction (RS) [9] algorithm, the relation result is folded by fractal

reconstruction to eliminate ambiguity, but the acquisition accuracy is declined caused by its wide main lobe. In Sub-Correlation Function (SCF) [10] algorithm, multiple kinds of local BOC signals are correlated with the received BOC signal, and a correlation function without side peaks is obtained, but it adopts the combination of multiplication so that the calculation is large. Typical frequency domain algorithms are as follows: BPSK-like [11]–[13] method is similar to the way of processing binary phase shift key (BPSK) signal, which treats BOC signal as the sum of two BPSK signals with different carrier frequencies, but it loses the advantage of high precision. In Single side band(SSB) [14] algorithm, two first-order BPSK components are regarded as two BPSK modulation signals, which are used for routine acquisition and detection, respectively. The acquisition algorithm based on Fast Fourier Transform (FFT) [15] does not rely on integral correlation of the local BOC signal and the received BOC signal, it uses FFT spectrum analysis to search the pseudo-random (PN) code phase and to estimate Doppler frequency in the frequency domain. However, it is difficult to satisfy synchronous sampling and integral period truncation in practice, Doppler frequency estimation is always disturbed by spectrum leakage and fence effect, which results in poor performance or even failure to synchronize. In the actual communication environment, due to the large radial velocity and radial acceleration between the satellite and the earth, the received signal is often coupled with thousands or even ten thousands Hz Doppler frequency [16], which is not seriously concerned in methods mentioned above and could lead to a reduction in the detection probability or even failed acquisition. Therefore, it is very necessary to study the acquisition problem for BOC modulated signals with large Doppler shift [17].

In this paper, all phase processing and cumulative average are applied to improve the system performance. A transform domain method combining all phase FFT (apFFT) spectrum analysis [18] and partial matched filter (PMF) is used to realize the acquisition of high dynamic BOC modulation signals. The organization of this paper is as follows. Section II formalizes the BOC modulated signal model, the exact expressions of the output of PMF-apFFT and the detection probability of the PMF-apFFT algorithm. Section III presents the specific process of the acquisition scheme and an efficient structure diagram for the proposed algorithm. In Section VI, the specific simulation parameters are abstracted firstly, the comparative simulations and the calculation of the proposed algorithm and PMF-FFT algorithms are shown and discussed. Finally, conclusions as well as the applications are discussed in Section V.

II. SIGNAL MODEL AND ACQUISITION PRINCIPLE
A. BOC MODULATED SIGNAL MODEL
Using the right-handed circular polarization antenna in receiver, BOC modulated signal is filtered by pre-filter and amplified by a low-noise amplifier. The radio frequency (RF)

signal is converted into an intermediate frequency (IF) signal by a down-conversion converter. The out-of-band noise and interference are filtered by an IF bandpass filter, the received BOC signal can be expressed as

$$r(t) = Ad(t)s(t)\cos((f_{IF} + f_d)t + \phi_0) + n(t) \quad (1)$$

where A is the amplitude of signal; $d(t)$ is navigation data; f_{IF} is intermediate frequency; f_d is Doppler shift; ϕ_0 is the initial phase of the carrier; $n(t)$ is White Gaussian noise with zero-mean and variance σ_n^2. $s(t)$ is BOC baseband signal and can be expressed as

$$s(t) = c(t)sc(t) \quad (2)$$

where $sc(t) = \mathrm{sgn}[\sin(2\pi f_{sc}t)]$ or $\mathrm{sgn}[\cos(2\pi f_{sc}t)]$, which is the subcarrier with the frequency f_{sc} and the period T_{sc}, $\mathrm{sgn}(x)$ is the sign function, which takes the value of 1 for x >0 and -1 for x < 0. $c(t)$ is the spreading code, can be expressed as

$$c(t) = \sum_{i=-\infty}^{\infty} c_i p_{T_c}(t - iT_c) \quad (3)$$

where $c_i \in \{-1, 1\}$ is the ith chip of a PN code, $p_\alpha(t)$ is the PN code waveform, which is a rectangular pulse over $[0, \alpha)$, T_c is the chip period of PN code.

B. PMF-FFT ACQUISITION SCHEME
BOC signal is generated by modulating navigation bit with PN code first and then modulating with subcarrier, which is similar with the source coding. The latter step can be completely carried out first, which is shown in Eq.(2), modulating PN code with subcarrier to generate BOC baseband signal, and then BOC baseband signal modulates navigate bit. After digital-to-analog, BOC signal with large Doppler shift is converted into digital signal, which can be written as

$$\begin{aligned} x(i) &= d(i)c(i)sc(i)\exp[j(2\pi f_d iT_c + \phi)] + n(i) \\ &= d(i)s(i)\exp[j(2\pi f_d iT_c + \phi)] + n(i) \quad (4) \end{aligned}$$

Obviously, $s(i)$ in Eq.(4) is only generated by modulating PN code with subcarrier, so all the properties of its PN code is not destroyed and is the same as the auto-correlation characteristics of traditional spread spectrum signal, and $s(i)$ can be defined as combined code. However, the combined code $s(i)$ is different from the traditional PN code, i.e., each chip is modulated with a subcarrier and becomes one or several square waves, whose duty cycle is 50 percent. Therefore, each "1" and "−1" in the subcarrier is used as the combined code chip and taken as a basic unit for sliding in acquisition.

In order to enlarge the parallel search range of Doppler frequency, sampling signal $x(i)$ and local combined code $s(i)$ are segmented, and each segmented $x'(i)$ is partially correlated with each segmented $s'(i + i')$ by PMF, i' is the delay between the local combined code and the received PN code. All sample points are filled with several zeros and cut into R parts, and each part has P points. For the convenience of analysis, the correlator output is divided into signal part and noise part. In the process of partial correlation, there is no

change in the navigate bit $d(t)$, i.e., the influence of $d(t)$ is not considered. The output of rth ($1 \leq r \leq R$) PMF is shown by

$$x^{'}(r) = s(r) + n(r) \qquad (5)$$

where $s(r)$ is the useful signal part, $n(r)$ is the noise part. And $s(r)$ can be expressed as

$$s(r) = \frac{1}{P} \sum_{i=(r-1)P+1}^{rP} s(i) s(i+i') \exp[j(2\pi f_d T_c + \phi)] \qquad (6)$$

As the phase of PN code in the received signal is equal with the phase of local combination code, there's a conclusion as follow

$$\sum_{i=(r-1)P+1}^{rP} s(i) s(i+i') = 1 \qquad (7)$$

So Eq.(6) can be rewritten as

$$\begin{aligned} s(r) &= \frac{1}{P} \sum_{i=(r-1)P+1}^{rP} \exp[j(2\pi f_d T_c + \phi)] \\ &= \frac{1}{P} \frac{\sin(\pi P f_d T_c)}{\sin(\pi f_d T_c)} \exp[j\pi f_d T_c (2rP - P) + \phi] \end{aligned} \qquad (8)$$

The FFT points are N, P must be filled with several zeros (P to N) to meet the requirement of 2-based FFT, then the output of FFT for the Eq.(8) is shown by

$$\begin{aligned} F(k) &= FFT\{s(r)\} = \sum_{r=1}^{R} s(r) * W_N^{rk} \\ &= \sum_{r=1}^{R} e^{j\pi f_d T_c (2rP-P)+\phi} \frac{\sin(\pi P f_d T_c)}{P \sin(\pi f_d T_c)} e^{-j\frac{2\pi}{N}rk} \\ &= \frac{1}{R} \cdot \frac{\sin(\pi P f_d T_c)}{P \sin(\pi f_d T_c)} \cdot \frac{\sin(\pi L f_d T_c - \pi R k/N)}{\sin(\pi P f_d T_c - \pi k/N)} \\ &\quad \cdot \exp(j\varphi(k, f_d)) \end{aligned} \qquad (9)$$

where $\varphi(k, f_d)$ is the phase characteristic of PMF-FFT, which can be expressed as

$$\varphi(k, f_d) = \pi (N-1)(P f_d T_c - k/N) - \pi f_d T_c (P-1) \qquad (10)$$

The normalized frequency response of Eq.(9) can be decomposed into the output of two parts, and the output of partial matching filter PMF is

$$G_{PMF}(f_d) = \frac{1}{P} \cdot \frac{\sin(\pi P f_d T_c)}{\sin(\pi f_d T_c)} e^{-j\pi f_d T_c (P-1)} \qquad (11)$$

The output of FFT module is

$$\begin{aligned} G_{FFT}(k, f_d) &= \frac{1}{N} \cdot \frac{\sin(\pi L f_d T_c - \pi R k/N)}{\sin(\pi P f_d T_c - \pi k/N)} \\ &\quad e^{j\pi(N-1)(P f_d T_c - k/N)} \end{aligned} \qquad (12)$$

$G_{FFT}(k, f_d)$ is caused by incomplete FFT phase compensation. If the maximum output value of $G_{FFT}(k, f_d)$ exceeds the threshold, the phase of received PN code and the phase of local combined code are preliminarily aligned, and Doppler

shift can be estimated by $f_d = k/(PNT_c)$ at the same time. However, when there is no positive integer k corresponding to a certain Doppler shift, the frequency leakage will occur in the kth frequency channel of FFT, and the output will be greatly attenuated, which is called fence effect.

C. PMF-apFFT ACQUISITION SCHEME

In signal processing, spectrum leakage caused by data truncation, and the solution is often to add Windows and spectrum correction. In this paper, all phase spectrum analysis is adopted to reduce the effect of truncation by overlapping. The BOC modulated signal is discretized and cut into R parts, each part has P points, and the result is shown by

$$\mathbf{x}_r(n) = \mathbf{x}[n + P(r-1)], \quad (0 \leq n \leq P), \quad (1 \leq r \leq R) \qquad (13)$$

Taking the first signal sequence as an example, i.e. $r = 1$, the output of apFFT can be derived. The sampling data x is written as row vector

$$\mathbf{x}(n) = \begin{bmatrix} x(1) & x(2) & x(3) \dots x(P) \end{bmatrix} \qquad (14)$$

$2M-1$ points data is required for M points all-phase processing, the processed data of length $2M - 1$ is divided into M segments, and the length of each segment is M. A $M * M$ data matrix $\mathbf{D}$ is given by all the truncation of central sampling data $x(M)$

$$\mathbf{D} = \begin{bmatrix} x(M) & x(M+1) & x(M+2) \dots & x(2M-1) \\ x(M-1) & x(M) & x(M+1) \dots & x(2M-2) \\ x(M-2) & x(M-1) & x(M) \dots & x(2M-3) \\ & & \vdots & \\ x(1) & x(2) & x(3) \dots & x(M) \end{bmatrix} \qquad (15)$$

The rows are moved to align with the center data $x(M)$ by cyclic shifting, the matrix $\mathbf{D}$ can be rewritten as

$$\mathbf{D} = \begin{bmatrix} x(M) & x(M+1) \dots & x(2M-2) & x(2M-1) \\ x(M) & x(M+1) \dots & x(2M-2) & x(M-1) \\ & \vdots & & \\ x(M) & x(2) \dots & x(M-2) & x(M-1) \\ x(M) & x(1) \dots & x(M-2) & x(M-1) \end{bmatrix} \qquad (16)$$

After windowing and adding by corresponding columns, the elements of result are defined as follows

$$\begin{aligned} \mathbf{x}_{ap}(1) &= x(M) \\ \mathbf{x}_{ap}(2) &= (M-1)x(M+1) + x(1) \\ &\vdots \\ \mathbf{x}_{ap}(M) &= (M-1)x(M-1) + x(2M-1) \end{aligned} \qquad (17)$$

A data row vector $\mathbf{x}_{ap}$ after all phase processing and normalizing can be expressed as

$$\begin{aligned} \mathbf{x}_{ap} &= \frac{1}{M} [Mx(M), (M-1)x(M+1) + x(1), \\ &\quad \cdots, x(2M-1) + (M-1)x(M-1)] \end{aligned} \qquad (18)$$

According to the homogeneity and superposition of FFT, the FFT result $X'_m(k)$ of each row vector in Eq. (16) can be derived from the FFT result $X_m(k)$ of each row vector in Eq. (15)

$$X'_m(k) = X_m(k) e^{j\frac{2\pi}{N}mk} m, \quad k = 0, 1, \cdots M-1 \quad (19)$$

Combining with Eq.18 and Eq.19, the output of PMF-apFFT is shown by(FFT points are N)

$$\begin{aligned}
X_{ap}(k) &= \frac{1}{N}\sum_{m=0}^{N-1} X'_m(k) = \frac{1}{N}\sum_{m=0}^{N-1} X_m(k)e^{j\frac{2\pi}{N}mk} \\
&= \frac{1}{N^2}\sum_{m=0}^{N-1}\sum_{r=0}^{N-1} x(r-m)e^{-j\frac{2\pi}{N}kr}e^{j\frac{2\pi}{N}mk} \\
&= \frac{1}{N^2}e^{-j\pi Pf_d T_c+\varphi}\cdot\frac{1}{P}\frac{\sin(\pi Pf_d T_c)}{\sin(Pf_d T_c)}\sum_{m=0}^{N-1} \\
&\quad e^{-j(2\pi Pf_d T_c-k)m/N} \\
&\quad \cdot\sum_{r=0}^{N-1} e^{j(2\pi Pf_d T_c-k)r/N} \\
&= \frac{1}{PN^2}\cdot e^{-\pi f_d(P-1)T_s+2\pi N(f_d PT_c-k/N)} \\
&\quad \cdot\frac{\sin(\pi Pf_d T_c)}{\sin(\pi f_d T_c)}\left|\frac{\sin(\pi Lf_d T_c-\pi Rk/N)}{\sin(\pi Pf_d T_c-\pi k/N)}\right|^2 \quad (20)
\end{aligned}$$

Using an equivalent of the modulus operator on the Eq.(20), frequency response of PMF-apFFT can be written as

$$\begin{aligned}
\left|G_{apFFT}(f_d, k)\right| &= \left|X_{ap}(k)\right|/\left(\max\left(\left|X_{ap}(k)\right|\right)\right) \\
&= \frac{1}{N^2}\left|\frac{\sin(\pi Pf_d T_c)}{P\sin(\pi f_d T_c)}\right|\cdot\left|\frac{\sin\left(\pi Lf_d T_c-\frac{\pi Rk}{N}\right)}{\sin\left(\pi f_d PT_c-\frac{\pi k}{N}\right)}\right|^2 \\
&= \frac{1}{N^2}\cdot G_1(f_d, k)\cdot G_2(f_d, k) \quad (21)
\end{aligned}$$

According to Eq.(21), the normalized output based on PMF-apFFT acquisition algorithm consists of $G_1(f_d, k)$ and $G_2(f_d, k)$. $G_1(f_d, k)$ is introduced by the accumulation of PMF, with the increase of Doppler shift, it results in periodic attenuation of FFT output, i.e. scallops loss, known as fan effect. And $G_1(f_d, k)$ has a maximum value when the Doppler shift $f_d = 0$, or the length of PMF $P = 1$. Fig. 2 is the simulation chart of Eq.(21) taking Doppler shift as x-axis and 8-point FFT, and the thickening part of the curve is the result of both fan effect and fence effect. $G_2(f_d, k)$ is caused by incomplete FFT phase compensation, and it can be seen from Eq.(9) and Eq.(21) that the compensation term of apFFT is the square of that of common FFT, and energy of the side lobe relative to energy of the main lobe is attenuated according to such a quadratic relationship, which is shown in Figure 1 and Figure 2. Therefore, apFFT has a good performance in reducing spectrum leakage. In addition, Eq.(21) is derived on the premise of PN code alignment, i.e., Doppler frequency of partial correlation signal is searched in N frequency channels when the phase of received PN code is equal with the phase of local combined
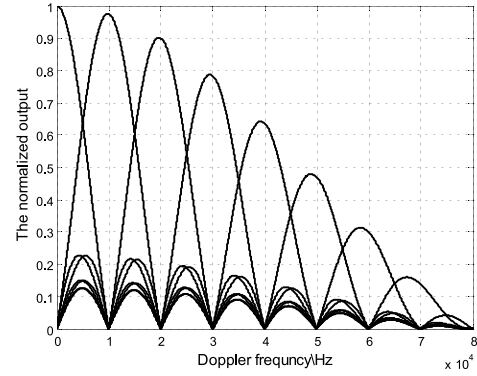

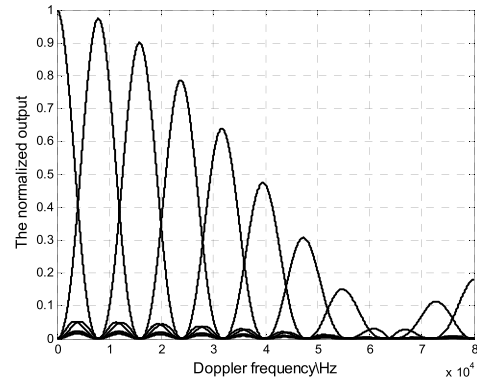**FIGURE 1.** The output of PMF-FFT with different doppler frequencies.

FIGURE 2. The output of PMF-apFFT with different doppler frequencies.

code. If there is a certain Doppler shift f_d, which meets $|\pi NPf_d T_c-\pi k| < \varepsilon$, where ε is any small positive number, a peak will appear in the kth frequency channel of apFFT.

In addition, cumulative averaging technique is implemented to reduce estimation variance to further improve the performance for weak BOC signals, so that the spectrum will not be buried in the noise and result in missing. The method is to divide the output of apFFT with the length of M into Q segments, and the length of each segment is X, i.e., $M = QX$, and can be written in vector form

$$\mathbf{X}_{ap} = \left[X_{ap1}(k), X_{ap2}(k), \cdots, X_{api}(k), \cdots, X_{apQ}(k)\right] \quad (22)$$

Adding up Q items in the vector and then averaging the result

$$\overline{\mathbf{X}_{ap}} = \sum_{i=1}^{Q}\frac{1}{Q}X_{api}(k) \quad (23)$$

Once the maximum value of Eq. (23) exceeds threshold, it is identified as the acquisition is completed and turn to tracking stage. In addition, an important property of apFFT spectrum analysis derived in [19] is that, after windowless apFFT and FFT, respectively, the ratio of their spectrum mean squares of Gaussian random noise is 2/3. In the other words, the average power of random noise after apFFT is smaller than that after FFT. Therefore, all phase processing

can effectively suppress Gaussian random noise, especially in the case of low signal-noise ratio (SNR).

D. DETECTION PROBABILITY

In the additive white Gaussian noise environment, false alarm and missed detection occur in the acquisition, H_0 denotes only noise signal, H_1 denotes the presence of useful signal. The probability of false alarm depends on the distribution characteristics of the input noise, and the output of a single frequency channel is subject to Rayleigh distribution after apFFT, its mean $m_a = 0$ and variance $\sigma^2 = (2N^2+1)\sigma_n^2/3N$, so the probability density function of single channel's output is shown by [20]

$$P_k(a) = \frac{a^2}{\sigma^2} \exp\left(-\frac{a^2}{2\sigma^2}\right), \quad a \geq 0 \tag{24}$$

Due to statistical independence for each channel, it is equivalent to the R-Tuple Bernoulli experiment, which is subject to the Binomial distribution, the probability of false alarm in the system can be expressed as

$$p_{fa} = 1 - \left[1 - p_k(\overline{X_{ap}} > V_T|H_0)\right]^R \tag{25}$$

The expression of threshold V_t can be obtained from Eq.(25)

$$V_t = \sqrt{-2L \ln\left[1 - \left(1 - p_{fa}\right)^{1/R}\right]} \tag{26}$$

And the probability of false alarm P_a in a single channel can be expressed as

$$P_a = \int_{V_t}^{+\infty} \frac{x^2}{\sigma^2} \exp\left(-\frac{a^2}{2\sigma^2}\right) da = \exp\left(-\frac{V_t^2}{2\sigma^2}\right) \tag{27}$$

At the output of the apFFT, the amplitude of the signals are taken, thus the statistics of the output of some apFFT bin k are Ricean, is given by

$$P_k(a) = \frac{a^2}{\sigma_n^2} \exp\left(-\frac{a^2 + m^2}{2\sigma_n^2}\right) I_0\left(\frac{am^2}{\sigma_n^2}\right), \quad a \geq 0 \tag{28}$$

where I_0 is the zero-order modified Bessel function, and m is the summation of the mean of the signals on the inphase and quadrature branches for bin k

$$m^2 = m_I^2 + m_Q^2 \tag{29}$$

The detection probability of the kth channel can be expressed as

$$P_d(k) = p_r\left(X_{ap}(k) > V_T|H_1\right)$$
$$= \int_{V_t}^{+\infty} P(a)da = Q(m/\sigma, V_t/\sigma)$$
$$= Q\left(\sqrt{6XN^2/\left(2N^2+1\right) \cdot SNR \cdot X_{ap}(k)},\right.$$
$$\left.\sqrt{-2\ln\left(1 - N\sqrt{1 - P_{fa}}\right)}\right) \tag{30}$$

where $Q(\cdot)$ is Marcumq function. Signal acquisition is assumed if any of the output bins is greater than the threshold. Each of the N FFT output bins have the same distribution, and therefore the probability of any one of the N outputs exceeding the threshold can be given by

$$P_d = 1 - \prod_{k=0}^{N-1}\left(1 - P_d(k)\right) \tag{31}$$

where P_d is detection probability of the proposed algorithm in the Gaussian channel.

III. THE STEPS OF PMF-apFFT ALGORITHM

Acquisition processes are as follows

(1) After down conversion and analog-digital conversion (ADC), the received BOC modulated signal with a length of L is sampled at the PN code rate and cut into R parts, each part has P points

(2) Local combined code is taken L points in order and cut into R parts, each part has P points

(3) The received BOC signal is correlated with the local combined code in segment by PMF, and R segments are completed successively.

(4) All phase processing was performed for the correlation results.

(5) The processing results are recombined to form a $R * P$ matrix $W(i, j)$, where i is the number of the correlator and j is the jth element in each correlator. Then N points FFT operation is done for each row of matrix W.

(6) The outputs of apFFT are arranged to obtain matrix $w(i, j)$, storing the result in the corresponding accumulator

(7) The maximum value of N accumulators is compared with the threshold, if the maximum value exceeds the threshold, it enters the tracking stage; if not, calculating the next row and compare

(8) If the row operation of the matrix is completed, there is still no value greater than the threshold, adjusting the local combined code by synchro-control module, and repeating the steps 3-7 until the value of peak exceeds the threshold.

Fig.3 describes the acquisition process of the proposed algorithm.

IV. SIMULATION AND RESULTS ANALYSIS

In this paper, in order to better suppress spectrum leakage caused by truncation, Hanning window is adopted in all phase spectrum analysis and traditional FFT spectrum analysis. In order to verify the performance of the proposed scheme, the acquisition for BOC modulation signal is simulated by MATLAB. The sine phased and cosine phased BOC signals are expressed as sBOC and cBOC, respectively. If no description, sBOC(1,1) modulated signal is simulated in additive white Gaussian noise channel, and simulation parameters are set as follows. The phase of PN code is 511, Doppler shift of the signal $f_d = 25$kHz after down-conversion, the PN code rate is 8.148MHz. The length of partial matched filter
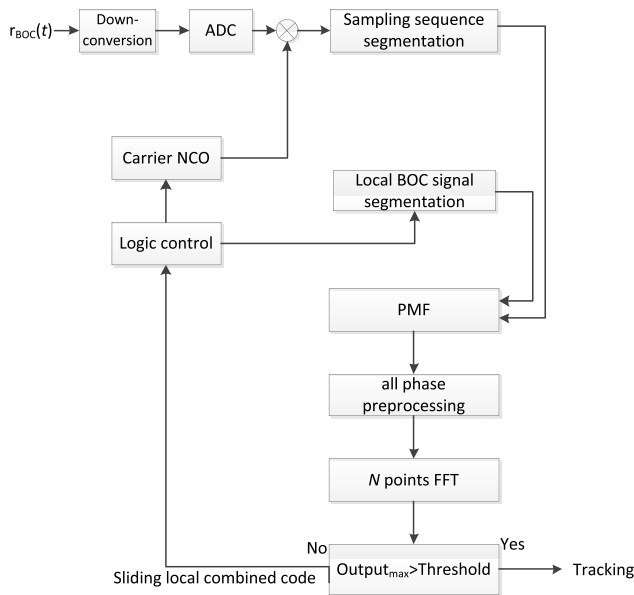
FIGURE 3. The block diagram of the proposed algorithm.
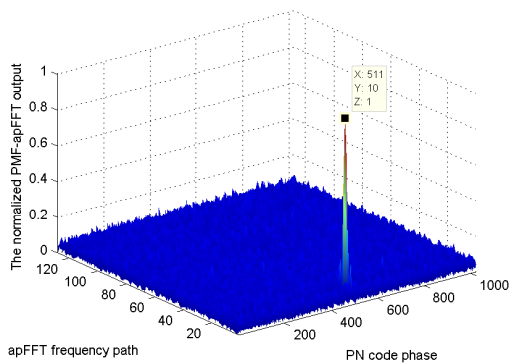

FIGURE 4. 2D acquisition diagram of PMF-apFFT algorithm.

$P = 255$, the number of partial matched filter $R = 4$, the period of BOC modulated baseband signal $L = P * R = 1020$, the number of FFT $N = 256$. According to $|\pi N P f_d T_c - \pi k| < \varepsilon$, $k = 10$. And integral time $T = 1$ms, false alarm probability $P_{fa} = 0.0001$.

A. THE SIMULATION OF PMF-APFFT ALGORITHM
The two-dimensional (2D) acquisition diagram of PMF-apFFT algorithm proposed in this paper at SNR $= -10$dB is shown in Figure 4. The acquisition diagram peaks at the coordinate (511,10), which is consistent with the previous set parameters, this proves that the proposed algorithm is effective for BOC signal acquisition.

In Figure 5, the normalized amplitude of PMF-apFFT algorithm and that of FFT algorithm are respectively obtained by 100 times simulation for averaging at SNR $= -10$ db. Comparing Figure 5a and Figure 5b, it can be seen that the main peak of PMF-apFFT algorithm is more obvious than the secondary peak, which makes it easier to detect the main peak correctly.
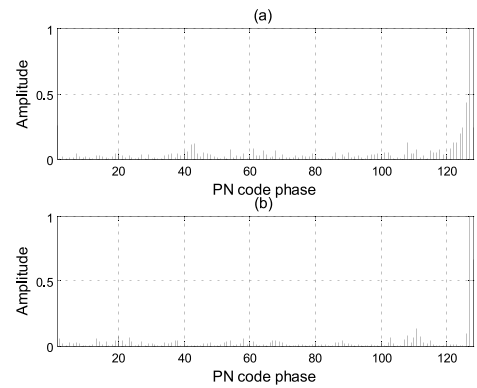

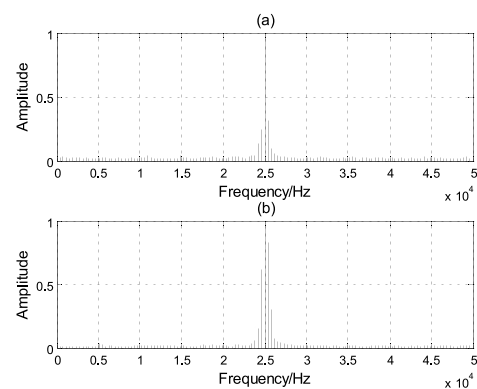**FIGURE 5. The normalized amplitudes of output. (a) PMF-apFFT algorithm. (b) PMF-FFT algorithm.**

FIGURE 6. The estimations of doppler shift. (a) PMF-apFFT algorithm. (b) PMF-FFT algorithm.

In Figure 6, Doppler shift estimation of apFFT algorithm and that of FFT algorithm are respectively obtained by 100 times simulation for averaging at SNR $= -10$ dB, and Doppler shift obtained from simulations is almost the same as the previous set with 25kHz. Similarly, the main peak of Doppler shift estimation of PMF-apFFT algorithm is easier to distinguish, which weakens the effect of large Doppler shift on acquisition.

B. FFT POINTS
In Figure 7, experiment shows that the proposed algorithm has good acquisition performance for high detection probability when FFT points is large enough. Compared with PMF-FFT algorithm, the proposed algorithm has higher detection probability with the same SNR. The simulation results in Figure 7 are consistent with the result of previous theoretical analysis, which is that the sidelobe attenuation rate of $G_{apFFT}(f_d, k)$ is slower.

Meanwhile, the detection probability varies greatly with the choice of FFT points N, the greater the length of PMF is, the more FFT points are and the less acquisition time is. However, it increases the correlation loss and leads to the decrease of maximum FFT output, and the impact on Doppler shift is also more sensitive, which leads to a decline
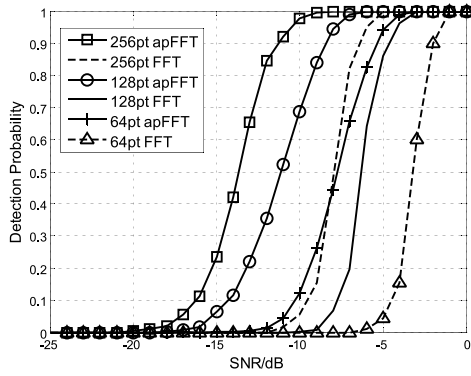
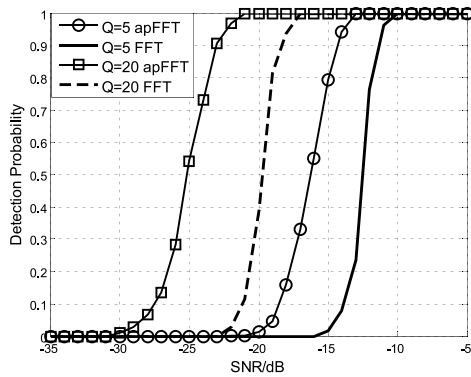**FIGURE 7.** Detection probabilities of PMF-apFFT algorithm and PMF-FFT algorithm for different FFT points.

FIGURE 8. Detection probabilities of PMF-apFFT algorithm and PMF-FFT algorithm for Q = 5 and Q = 20.

in detection probability. On the other hand, the smaller the correlation length is, the smaller the correlation loss will be, but it increases the number of PMF, resulting in higher hardware requirements [21]. Therefore, the appropriate FFT points should be selected according to the requirements of acquisition time and precision in the receiver.

C. CUMULATIVE AVERAGING TECHNIQUE
As FFT points $N = 256$ and the cumulative frequency is equal to 5 and 20 respectively, after 5000 times Monte Carlo simulations, detection probabilities of PMF-apFFT and PMF-FFT algorithm are shown in Figure 8. When the detection probability is 1, accumulating from 5 times to 20 times, SNR is improved about 8dB by PMF-apFFT algorithm and 7dB by PMF-FFT algorithm. Under the same SNR, with the increasing cumulative frequency, the higher detection probability is, thus cumulative averaging technique adopted in this paper can further improve the acquisition performance in low SNR environment.

D. DETECTION PROBABILITIES OF DIFFERENT ALGORITHMS FOR sBOC(2,1) and cBOC(1,1)
In order to evaluate the performance of the proposed algorithm more comprehensively, detection probabilities of PMF-FFT, PCF, SR, ACF and PMF-apFFT algorithm for
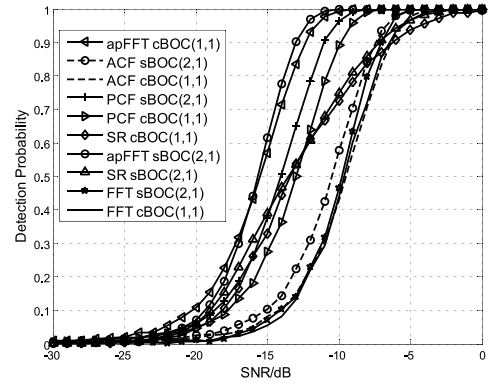

FIGURE 9. Detection probabilities of PMF-apFFT, PMF-FFT, PCF,SR and ACF algorithm for sBOC(2,1) and cBOC(1,1).

sBOC(2,1) and cBOC(1,1) are assessed by Monte Carlo simulation in Figure 9, respectively. Whether for sBOC(2,1) or cBOC(1,1), detection probability of the proposed algorithm approximately reaches 1 at SNR= −10dB, which is better than that of other algorithms. And the proposed algorithm is suitable for both sine- and cosine- BOC signals with any modulation order.

E. THE EFFECT OF DOPPLER SHIFT ON THE ACQUISITION
When $f_d = 0$, 25kHz, 40kHz, detection probabilities of PMF-apFFT, PMF-FFT, PCF and SR algorithm are shown in Figure 10. Obviously, detection probability of PMF-apFFT algorithm is always greater than that of other algorithms with same Doppler shift and same SNR. Compared with PMF-FFT algorithm, SNR of PMF-apFFT algorithm improves 5dB with $f_d = 40$kHz and 3dB with $f_d = 25$kHz, respectively. In addition, detection probabilities of PCF algorithm and SR algorithm are always 0 when $f_d = 25$kHz, which means that the system is no longer in working condition. On the one hand, the search range of Doppler shift is effectively expanded by the proposed algorithm [22]. On the other hand, all truncation conditions of central data are considered with all-phase processing, which reduces the compensation error of Doppler shift, and then weakens the distortion of correlation peak caused by large Doppler shift. Thus, the proposed algorithm is especially applicable in the case of large Doppler shift.

F. WINDOWS
The spectrum leakage is closely related to the sidelobe of the window function spectrum, if amplitude of the sidelobe is close to zero, the energy is relatively concentrated in the main lobe, which makes it close to the real spectrum. Therefore, different window functions can be used to intercept the signal in all phase processing to solve the problem of spectrum leakage. Comparison of the effect of Blackman window and Hanning window is shown in Figure 11, in the case of the same window function, the detection probability of PMF-apFFT algorithm is always greater than that of PMF-FFT algorithm. In addition, windowing greatly reduces the spectrum leakage
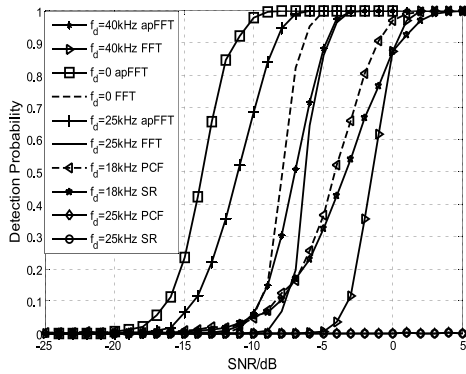
FIGURE 10. Detection probabilities of PMF-apFFT, PMF-FFT, PCF and SR algorithm for $f_d = 0$, 18kHz, 25kHz, 40kHz.
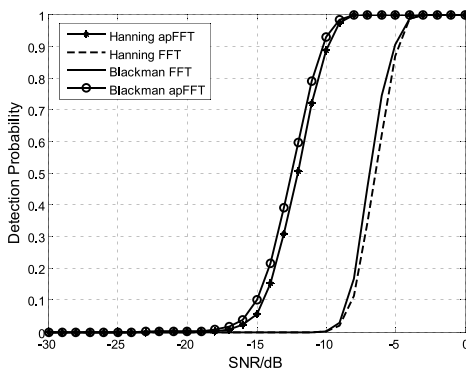

FIGURE 11. Detection probabilities of PMF-apFFT algorithm and PMF-FFT algorithm with hanning and blackman window.

and increases the peak directly. Moreover, the effect of Blackman window is better than that of Hanning window.

G. CALCULATION AND HARDWARE REQUIREMENT

The difference between apFFT and FFT is all-phase processing, which is added to the data before FFT. Therefore, compared with FFT, more calculation is on the windowing and summation of data in all phase processing, and windowless apFFT only carries out $M(M-1)$ real addition to data. In general, for M points apFFT, double window, single window and windowless apFFT all do approximately M^2 more real addition than FFT, and they do the same amount of complex multiplication and addition, which are shown in Table.1. Due to the calculation of single addition is much smaller than that of single multiplication, so the added amount of real addition operations is small compared with the total amount of computation. In addition, $2M-1$ points data is required for M points apFFT and segmented from back to front, so apFFT cannot be carried out until $2M-1$ data is in place, and FFT can be carried out as long as M data are in place, so apFFT requires almost twice as much storage as that of FFT. In addition, compared with PCF algorithm and SR algorithm, FFT points of the proposed algorithm are reduced and the number of filters is increased in the practical operation. Taken together,

TABLE 1. The calculations of FFT and windowless apFFT.

Algorithm	data length	Ord-er	Complex multiplication	Complex addition	Real addition
FFT	M	M	$(M/2)\log 2M$	$M\log_2 M$	-
Windowle-ss apFFT	$2M$-1	M	$(M/2)\log 2M$	$M\log_2 M$	$M(M$-1$)$

the increased hardware cost is acceptable in the consideration of good performance of the proposed algorithm.

V. CONCLUSION

In this paper, a novel acquisition algorithm based on PMF-apFFT for BOC modulated signal is proposed. The received BOC signal was partially correlated with local BOC signal by PMF, after apFFT and cumulative averaging, the result was compared with threshold to determine whether the acquisition was successful or not. Experiment results and simulation analysis show that detection probability of PMF-apFFT algorithm is much better than that of PMF-FFT, PCF and SR algorithm in the same simulation conditions. Due to the superior performance of PMF-apFFT, spectrum leakage is minimized, which greatly improves the accuracy of Doppler frequency estimation, the increased hardware cost and calculation are acceptable. The proposed algorithm is applicable to the complex communication environment with strong noise and large Doppler shift. And the future research direction is to reduce the calculation and hardware cost of PMF-apFFT algorithm.

ACKNOWLEDGMENT

REFERENCES

[1] Y. Yang, X. Ba, and J. Chen, "A novel VLSI architecture for multi-constellation and multi-frequency GNSS acquisition engine," *IEEE Access*, vol. 7, pp. 655–665, 2019.

[2] H. Xiong, S. Wang, S. Gong, M. Peng, J. Shi, and J. Tang, "Improved synchronisation algorithm based on reconstructed correlation function for BOC modulation in satellite navigation and positioning system," *IET Commun.*, vol. 12, no. 6, pp. 743–750, Apr. 2018.

[3] G. Yang, Z. Yao, and M. Lu, "Theoretical analysis of unambiguous 2-D tracking loop performance for band-limited BOC signals," *GPS Solutions*, vol. 22, no. 1, p. 30, 2018.

[4] C. Sun, H. Zhao, W. Feng, and S. Du, "A frequency-domain multipath parameter estimation and mitigation method for BOC-modulated GNSS signals," *Sensors*, vol. 18, no. 3, p. 721, 2018.

[5] C. J. Guo, B. Xu, and Z. Tian, "Research on multi-constellation GNSS compatible acquisition strategy based on GPU high-performance operation," *EURASIP J. Wireless Commun. Netw.*, vol. 1, p. 112, Dec. 2018.

[6] D.-S. Shim and J.-S. Jeon, "An unambiguous delay-and-multiply acquisition scheme for GPS L1C signals," *Sensors*, vol. 18, no. 6, p. 1739, 2018.

[7] O. Julien, C. Macabiau, M. E. Cannon, and G. Lachapelle, "ASPeCT: Unambiguous sine-BOC(n,n) acquisition/tracking technique for navigation applications," *IEEE Trans. Aerosp. Electron. Syst.*, vol. 43, no. 1, pp. 150–162, Jan. 2007.

[8] Z. Yao, X. Cui, M. Lu, Z. Feng, and J. Yang, "Pseudo-correlation-function-based unambiguous tracking technique for sine-BOC signals," *IEEE Trans. Aerosp. Electron. Syst.*, vol. 46, no. 4, pp. 1782–1796, Oct. 2010.

[9] T. Q. Zhang, Z. Yan, X. Ou, and W. Qian, "Acquisition algorithm combining parallel code phase with fractal reconstruction of TMBOC modulation signal," *J. Shanghai Jiaotong Univ.*, vol. 50, no. 5, pp. 782–787, 2016.

[10] S. Kim, D. Chong, and S. Yoon, "A new GNSS synchronization scheme," in *Proc. IEEE 69th Veh. Technol. Conf.*, Apr. 2009, pp. 1–5.

[11] E. S. Lohan, "Statistical analysis of BPSK-like techniques for the acquisition of Galileo signals," *J. Aerosp. Comput., Inf., Commun.*, vol. 3, no. 5, pp. 234–243, 2006.

[12] N. Martin, V. Leblond, G. Guillotel, and V. Heiries, "BOC (x,y) signal acquisition techniques and performances," in *Proc. 16th Int. Tech. Meeting Satell. Division Inst. Navigat. (ION GPS/GNSS)*, 2003, pp. 188–198.

[13] P. M. Fishman and J. W. Betz, "Predicting performance of direct acquisition for the M-code signal," in *Proc. Nat. Tech. Meeting Inst. Navigat.*, 2000, pp. 574–582.

[14] P. Blunt, "Advanced global navigation satellite system receiver design," Ph.D. dissertation, Univ. Surrey, Guildford, U.K., 2007.

[15] Y. Zhang, W. Lu, and D. Yu, "A fast acquisition algorithm based on FFT for BOC modulated signals," in *Proc. IEEE Region 10 Conf. (TENCON)*, Nov. 2015, pp. 1–6.

[16] Y. Luo, L. Zhang, and N. El-Sheimy, "An improved DE-KFL for BOC signal tracking assisted by FRFT in a highly dynamic environment," in *Proc. IEEE/ION Position, Location Navigat. Symp. (PLANS)*, Apr. 2018, pp. 1525–1534.

[17] P. Tang, X. Li, and S. Wang, "A differential weighted accumulation algorithm using variable sliding window," *IEEE Access*, vol. 6, no. 1, pp. 21220–21230, 2018.

[18] J. Tian, J. Sun, G. Wang, Y. Wang, and W. Tan, "Multiband radar signal coherent fusion processing with IAA and apFFT," *IEEE Signal Process. Lett.*, vol. 20, no. 5, pp. 463–466, May 2013.

[19] X. D. Huang, Z. H. Wang, and P. Luo, "Discrimination and correction for dense all-phase FFT spectrums," *Acta Electronica Sinica*, vol. 39, no. 1, pp. 172–177, 2011.

[20] X. D. Huang and Z. H. Wang, "Anti-noise performance of all-phase FFT phase measuring method," *J. Data Acquisition Process.*, vol. 26, no. 3, pp. 286–291, 2011.

[21] H. Hou, K. Wu, Y. Chen, and X. Liang, "A new rapid and accurate synchronization scheme based on PMF-FFT for high dynamic GPS receiver," *IEICE Trans. Fundam. Electron., Commun. Comput. Sci.*, vol. 100, no. 12, pp. 3075–3080, 2017.

[22] S. M. Spangenberg, I. Scott, S. McLaughlin, G. J. R. Povey, D. G. M. Cruickshank, and P. M. Grant, "An FFT-based approach for fast acquisition in spread spectrum communication systems," *Wireless Pers. Commun.*, vol. 13, no. 1, pp. 27–55, 2000.
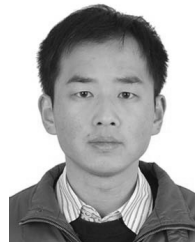
TIANQI ZHANG was born in 1971. He received the B.S. degree in physics from the Southwest University of China, in 1994, the M.S. degree in communication and electronic system, and the Ph.D. degree in circuits and systems from the University of Electronic Science and Technology of China, in 1997 and 2003, respectively. From 2003 to 2005, he was a Postdoctoral Fellow with Tsinghua University, and majors in communication and information system. Since 2005, he has been a Professor with the School of Communication and Information Engineering, Chongqing University of Posts and Telecommunications. His research interests include communication, and image and speech signal processing.

GANG ZHANG was born in 1976. He received the Ph.D. degree from the College of Communication Engineering, Chongqing University, Chongqing, in 2009. He is currently an Associate Professor with the Chongqing University of Posts and Telecommunications. His research interests include chaotic synchronization, chaotic secure communication, and weak signal detection.

YI PAN was born in 1988. He received the B.S. and M.S. degrees in signal and information processing from the Chongqing University of Posts and Telecommunications, in 2011 and 2014, respectively, where he is currently pursuing the Ph.D. degree in signal and information processing. His research interests include spread spectrum signal detection and processing, acquisition, tracking of BOC signal, and interference mitigating.

ZHONGTAO LUO received the M.S. degree in electronic engineering and the Ph.D. degree in signal and information processing from the University of Electronic Science and Technology of China, Chengdu, in 2007 and 2015, respectively. He is currently a Lecturer with the Chongqing University of Posts and Telecommunications. His research interests include statistical signal processing, array signal processing, and their applications in radar and communication systems.

• • •